Journal of Food and Drug Analysis, Vol. 14, No. 2, 2006, Pages 159-165 藥物食品分析 第十四卷 第二期

Characterization of Mouse Cytochrome P450-catalyzed Oxidative Metabolism of Rutaecarpine, an Alkaloid in the Herbal Medicine *Evodia rutaecarpa*

WOAN-CHING JAN[1,2,3], MING-JAW DON[1], LI-KANG HO[2], CHIEH-FU CHEN[1] AND YUNE-FANG UENG[1,2,4]*

[1.] *National Research Institute of Chinese Medicine, 155-1, Sec. 2, Li-Nong St., Taipei 112, Taiwan, R.O.C.*

[2.] *Department of Pharmacology, National Yang-Ming University, Taipei, Taiwan, R.O.C.*

[3.] *Mackay Medicine, Nursing and Management College, Taipei, Taiwan, R.O.C.*

[4.] *Graduate Institute of Medical Sciences, Taipei Medical University, Taipei, Taiwan, R.O.C.*

(Received: October 17, 2005; Accepted: December 21, 2005)

ABSTRACT

The alkaloid rutaecarpine exhibits antithrombotic and vasorelaxant effects. To characterize mouse cytochrome P450 (P450, CYP)-catalyzed rutaecarpine hydroxylations, the induction, inhibition, and kinetic properties of rutaecarpine hydroxylations were determined using liver microsomes of C57BL/6J mice. In untreated mice, rutaecarpine 10-, 11-, 12-, and 3-hydroxylation had K_m and V_{max} values ranging, respectively, between 11.6~16.7 μM and 62~197 pmol/min/mg protein. The formation rates of the four hydroxylated metabolites were inhibited by α-naphthoflavone and orphenadrine, but not by either sulfaphenazole or ketoconazole. 3-Methylcholanthrene-treatment increased rutaecarpine 11-, 12-, and 3-hydroxylation activities. Phenobarbital-treatment increased rutaecarpine 10-, 11-, 12-, and 3-hydroxylation activities. Dexamethasone had no effect on these hydroxylation reactions in mice. These results indicated that CYP1A and CYP2B, but not CYP3A, play major roles in rutaecarpine hydroxylations in mice.

Abbreviations: CYP, cytochrome P450; 3-MC, 3-methylcholanthrene; G6P, glucose-6-phosphate; α-NF, α-naphthoflavone; β-$NADP^+$, β-nicotinamide adenine dinucleotide phosphate.

Key words: rutaecarpine hydroxylation, cytochrome P450, mice, liver

INTRODUCTION

Rutaecarpine is a main quinazolinocarboline alkaloid isolated from *Evodia rutaecarpa* (Wu-chu-yu), which is used as a herbal medicine in the treatment of gastrointestinal disorders and headaches[1,2]. Pharmacological effects attributed to rutaecarpine include antithrombotic, antianoxic, hypotensive, and vasorelaxant[3]. Microsomal cytochrome P450 (P450, CYP)-dependent monooxygenase is the main enzyme system responsible for the oxidative metabolism of a variety of endogenous and xenobiotic compounds including natural products[4]. The resulting metabolites may show adverse effects or either cause a reduction or enhancement in parent compound pharmacological activity. *In vitro*, rutaecarpine is a CYP1A2-selective inhibitor in mouse and human liver microsomes without preincubation with NADPH[5]. Iwata *et al*. (2005) reported that rutaecarpine was a mechanism-based inhibitor of human CYP3A[6]. *In vivo*, oral treatment of mice with rutaecarpine significantly increased CYP1A2 protein level and catalytic activity in mice[7]. These results demonstrated interaction between rutaecarpine and P450. However, mouse liver microsomal metabolites of rutaecarpine were not identified and metabolic rates were not reported.

Rutaecarpine was metabolized using rat liver microsomal enzymes to form 10-, 11-, 12-, and 3-hydroxyr utaecarpine[8]. The formation rate of the total rutaecarpine metabolites was enhanced following treatments with 3-methylcholanthrene (3-MC) and phenobarbital but was unaffected following treatments with dexamethasone and acetone[9]. In both rats and mice, 3-MC, phenobarbital, acetone, and dexamethasone are prototypic inducers of CYP1A, CYP2B, CYP2E1, and CYP3A, respectively[10-12]. These results suggest that CYP1A and CYP2B play main roles in the metabolism of rutaecarpine in rats. However, quantification and kinetic analyses of rutaecarpine metabolite formation were not investigated. α-Naphthoflavone (α-NF), orphenadrine, sulfaphenazole, and ketoconazole are, respectively, inhibitors of CYP1A, CYP2B, CYP2C, and CYP3A[13,14]. Thus, we have studied the effects of P450 inhibitors and inducers on rutaecarpine oxidation to identify main mouse P450 forms involved in each metabolite formation. Hydroxyrutaecarpines were synthesized to perform quantification and kinetic analyses.

MATERIALS AND METHODS

I. *Chemicals*

Rutaecarpine was synthesized using the method

* Author for correspondence. Tel: +886-2-2820-1999 ext. 6351; Fax: +886-2-2826-4266; E-mail: ueng@nricm.edu.tw

described by Bergman and Bergman (1985)[15]. Disodium dexamethasone 21-phosphate, glucose-6-phosphate (G6P), G6P dehydrogenase, ketoconazole, 3-MC, 4-methylpyrazole, α-NF, β-nicotinamide adenine dinucleotide phosphate (β-$NADP^+$), orphenadrine, sodium phenobarbital, quinidine, and sulfaphenazole were purchased from Sigma-Aldrich Inc. (St. Louis, MO, USA). Metabolites, 3-, 10-, 11-, and 12-hydroxyrutaecarpine were synthesized from corresponding methoxyrutaecarpines as described in a previous report[8].

II. *Microsomal Preparation*

All experimental protocols involving animals were reviewed and approved by the Institutional Animal Care and Use Committee of the National Research Institute of Chinese Medicine. Male C57BL/6J mice (5 weeks old, weighing 13~16 g) were purchased from the National Laboratory Animal Center, Taipei. Before experimentation, mice were allowed a one-week acclimation period at the animal quarters with air conditioning, free access to commercial food pellets and an automatically controlled photoperiod of 12 hr light daily. 3-MC was dissolved in corn oil. Mice were treated with a single injection of 80 mg/kg 3-MC intraperitoneally. Liver microsomes were prepared after 48 hr. Phenobarbital and dexamethasone were dissolved in 0.9% sodium chloride. Mice were treated with 80 mg/kg/day phenobarbital or 30 mg/kg/day dexamethasone intraperitoneally for four days. Liver microsomes were prepared 24 hr after the final injection. Mouse liver microsomes were prepared by differential centrifugation at 4°C[16]. Microsomal pellets were stored at -75°C and microsomal activities were determined within two weeks.

III. *Enzyme Assays*

Microsomal protein concentration was determined by the method of Lowry *et al*. (1951)[17]. P450 content was determined by the spectrophotometric method described by Omura and Sato (1964)[18]. Rutaecarpine hydroxylation activity was determined as described above[8]. Each 1 mL incubation mixture contained 50 mM potassium phosphate buffer, pH 7.4, 5 mM $MgCl_2$, 1 mg/mL microsomal protein, a NADPH-generating system, and various concentrations of rutaecarpine as indicated in the results. The NADPH-generating system consisted of 13.7 mM G6P, 0.7 mM NADP, and 0.25 U/mL G6P dehydrogenase. Reaction was performed in a 37°C water bath with shaking for 20 min. Hydroxylation metabolites were separated through HPLC using an Extend-C18 column (4.6 × 250 mm, 5 μm, Agilent, USA) and detected by measuring the absorbance at 344 nm[8]. The amounts of hydroxyrutaecarpines were determined using synthetic standards. Orphenadrine and 4-methylpyrazole were dissolved in water. α-NF, sulfaphenazole, quinidine, and ketoconazole were dissolved in ethanol. For the inhibition study, the concentrations of α-NF, orphenadrine, sulfaphenazole, and ketoconazole were 10, 500, 10, and 1 μM in the assay, respectively. Inhibitors were added simultaneously with rutaecarpine into the incubation mixture. The final concentration of ethanol was lower than 0.4%.

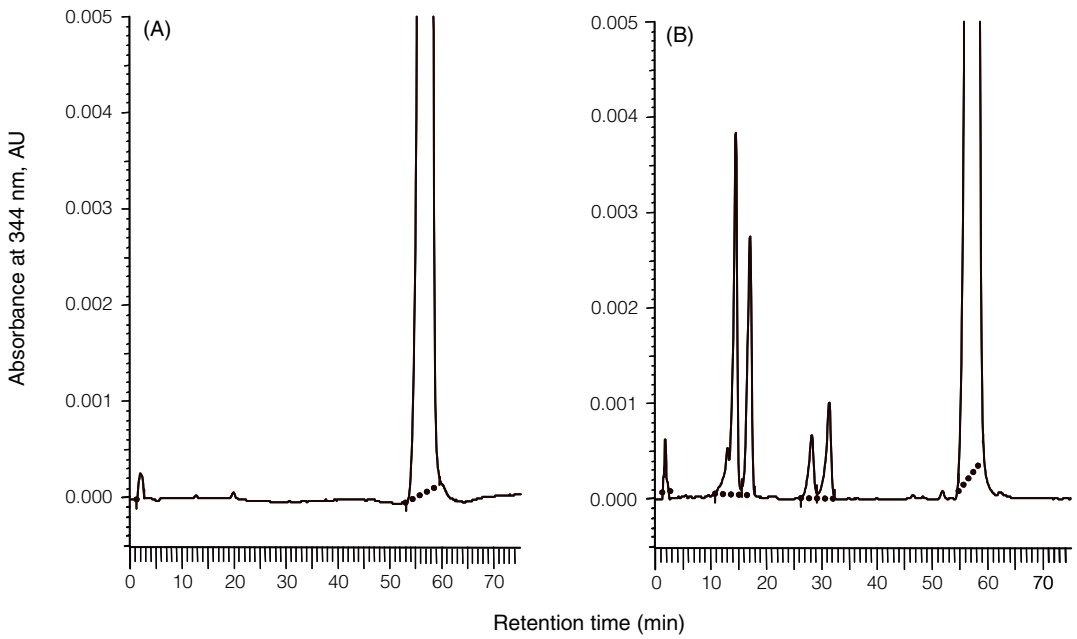

Figure 1. The HPLC chromatogram of rutaecarpine hydroxylations by mouse liver microsomes. Liver microsomes were prepared from untreated mice as described in the Materials and Methods section. Incubation was performed in the absence (A) and presence (B) of a NADPH-generating system. The metabolites 10-, 11-, 12-, and 3-hydroxyrutaecarpine appeared at 15, 17, 28, and 31 min, respectively. Rutaecarpine appeared at 57 min.

Journal of Food and Drug Analysis, Vol. 14, No. 2, 2006

IV. *Data and Statistical Analyses*

Kinetic analysis of mouse microsomal activity was performed by fitting velocity (v) values at various substrate concentrations (S) by unweighted nonlinear least-squares regression in accordance with the Michaelis-Menten equation: $v = V_{max}*S/(K_m \pm S)$, where V_{max} equals the maximal velocity (Sigma Plot, Jandel Scientific, San Rafael, CA, USA). Variance estimates (denoted as ± internal estimates of error) were derived from an analysis of individual datasets. The statistical significance of differences between control and treated groups was evaluated using the Student's t-test (Excel 2003, Microsoft Co., IL, USA), with a p value of < 0.05, considered to be statistically significant.

RESULTS

The four metabolites detected in the HPLC chromatogram of rutaecarpine metabolites in mice included 10-, 11-, 12-, and 3-hydroxyrutaecarpine (Figure 1). To determine the linear range of microsomal protein concentrations in rutaecarpine hydroxylation assay, researchers measured hydroxylation activity using various concentrations of microsomal proteins in the incubation mixture. Rutaecarpine 10-, 11-, 12-, and 3-hydroxylation activities were in a linear relationship with protein concentrations in the range of 0.5-1.2 mg/mL in the assay ($r \geq 0.99$) (Figure 2). Thus, in the following studies, 1 mg/mL microsomal protein was added to the rutaecarpine hydroxylation assay.

The major rutaecarpine oxidation products in untreated mouse liver microsomes were 10- and 11-hydroxyrutaecarpine (Table 1), with the formation rate of 10-hydroxyrutaecarpine significantly higher than that of 11-hydroxyrutaecarpine. Kinetic analysis revealed that these hydroxylations followed Michaelis-Menten reaction properties (Figure 3). The plot of rutaecarpine concentration versus the formation rates of rutaecarpine hydroxylation metabolites showed a hyperbolic pattern and the Lineweaver-Burk plot of the formation rates of rutaecarpine hydroxylation metabolites was in good linearity ($r = 0.99$). The V_{max} values generated by nonlinear regression analysis for 10-, 11-, 12-, and 3-hydroxylation were 197, 177, 62, and 65 pmol/min/mg protein, respectively (Table 1). The K_m values for 10-, 11-, 12-, and 3-hydroxylation were 11.6, 11.8, 16.7, and 12.0 μM, respectively. We used 200 μM rutaecarpine in the following assays of liver microsomes to reach saturated substrate concentration.

In the inhibition study, α-NF, a CYP1A inhibitor caused 59%, 70%, 74%, and 68% decreases of 10-, 11-, 12-, and 3-hydroxyrutaecarpine formation rates, respectively (Table 2). Orphenadrine, a CYP2B inhibitor, caused 46%, 45%, 53%, and 39% decreases of 10-, 11-, 12-,

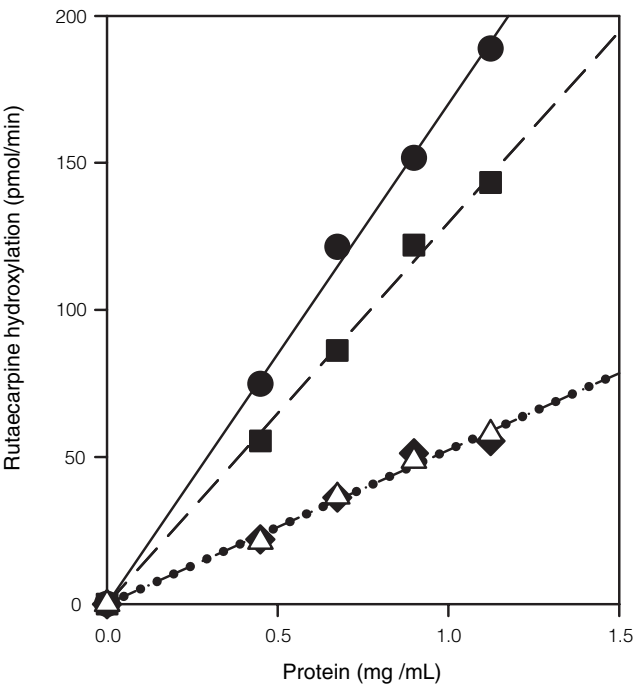

Figure 2. The relationships between rutaecarpine hydroxylation and protein concentrations in mouse liver microsomes. The formation rates of metabolites, 10-hydroxyrutaecarpine (●), 11-hydroxyrutaecarpine (■), 12-hydroxyrutaecarpine (◆), and 3-hydroxyrutaecarpine (Δ) were determined using 200 μM rutaecarpine. Results represent the means of duplicate determinations. Lines represent the lines of best fit as determined by linear regression analysis.

Table 1. Rutaecarpine hydroxylation activity of mouse liver microsomes

Reaction	Activity[a] pmol/min/mg protein	Kinetic parameters	
		K_m μM	V_{max} pmol/min/mg protein
10-Hydroxylation	159 ± 11[b]	11.6 ± 1.5	197 ± 5
11-Hydroxylation	114 ± 7	11.8 ± 1.2	177 ± 3
12-Hydroxylation	41 ± 3	16.7 ± 1.6	62 ± 1
3-Hydroxylation	38 ± 3	12.0 ± 1.7	65 ± 2

[a]Liver microsomal activities were determined at 200 μM rutaecarpine as described in the Materials and Methods section. Results represent the mean ± SEM for five mice.

[b]Rutaecarpine 10-hydroxylation activity was significantly higher than 11-hydroxylation activity as analyzed using a Student's t-test, $p < 0.05$. Kinetic parameters were calculated using a non-linear least-squares regression as described in the Materials and Methods section. The internal estimates of error (denoted as ±) are presented from analysis of individual sets of data with duplicated determinations.

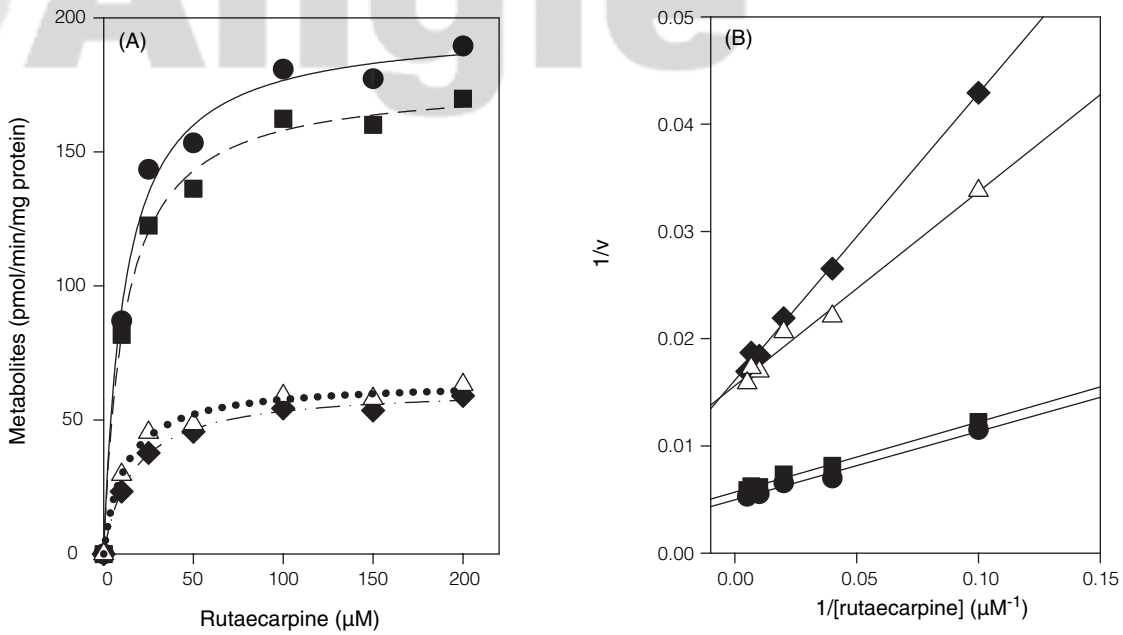

Figure 3. (A) Plot of rutaecarpine concentration against the formation rates of rutaecarpine hydroxylation metabolites, 10-hydroxyrutaecarpine (●), 11-hydroxyrutaecarpine (■), 12-hydroxyrutaecarpine (◆), and 3-hydroxyrutaecarpine (Δ). Results represent the means of duplicate determinations. Lines show the best fit as determined by nonlinear least-squares regression. (B) The Lineweaver-Burke plot of the formation rates of rutaecarpine hydroxylation metabolites, 10-hydroxyrutaecarpine (●), 11-hydroxyrutaecarpine (■), 12-hydroxyrutaecarpine (◆), and 3-hydroxyrutaecarpine (Δ). Lines show the best fit as determined by linear regression.

Table 2. Effects of CYP inhibitors on rutaecarpine hydroxylation activity in mouse liver microsomes

Inhibitor	% of control			
	10-hydroxyrutaecarpine	11-hydroxyrutaecarpine	12-hydroxyrutaecarpine	3-hydroxyrutaecarpine
α-Naphthoflavone (n = 5)	41 ± 5	30 ± 5	26 ± 6	32 ± 7
Orphenadrine (n = 3)	54 ± 8	55 ± 7	47 ± 2	61 ± 8
Sulfaphenazole (n = 3)	83 ± 5	81 ± 11	98 ± 12	80 ± 8
Ketoconazole (n = 5)	89 ± 10	93 ± 11	92 ± 6	99 ± 14

Results represent mean ± SEM of mouse liver microsomes. The number of mice (n) is shown in parenthesis. Rutaecarpine concentration was 200 μM in the assay. The concentrations of inhibitors used in the assays were described in the Materials and Methods section.

and 3-hydroxyrutaecarpine formation rates, respectively. However, the CYP2C inhibitor, sulfaphenazole caused decreases of less than 20% in hydroxyrutaecarpine formation rates and the CYP3A inhibitor ketoconazole had no effects on rutaecarpine hydroxylations.

In the induction study, microsomal rutaecarpine 10-hydroxylation activity was raised by 67% with phenobarbital-treatment (Figure 4); 11-hydroxylation activity by 42% and 53%, respectively, with 3-MC and phenobarbital treatments; 12-hydroxylation activity by 600% and 31%, respectively, with 3-MC and phenobarbital treatments; and 3-hydroxylation activity by 33% and 49%, respectively, with 3-MC and phenobarbital. Dexamethasone was found to have no effect on these hydroxylation activities.

DISCUSSION

It is recognized that species differences occur among xenobiotic-metabolizing P450 enzymes[19]. For example, the metabolic profiles in rats, mice and humans may show differences in regio-, enantio-, and stereo-selectivities. Our previous report demonstrated that rutaecarpine was oxidized by rat liver microsomes to form 10-, 11-, 12-, 3-hydroxyrutaecarpine[8]. 11-Hydroxyrutaecarpine was the most abundant metabolite in untreated rats. In mice, 10- and 11-hydroxyrutaecarpine were the principal microsomal oxidation metabolites of rutaecarpine (Table 1 and Figure 1). This research is the first to show a quantitative determination for rutaecarpine oxidation metabolites in mice. Mouse livers showed higher activity levels of 10-hydroxylation than 11-hydroxylation, suggesting that the metabolic profile of rutaecarpine does differ between species. Beside the species differences, humans show individual metabolic variations caused by genetic polymorphism, smoking, diet, and other endogenous and environmental factors. Thus, it will be of interest in the future to determine rutaecarpine hydroxylation in human liver samples.

Journal of Food and Drug Analysis, Vol. 14, No. 2, 2006

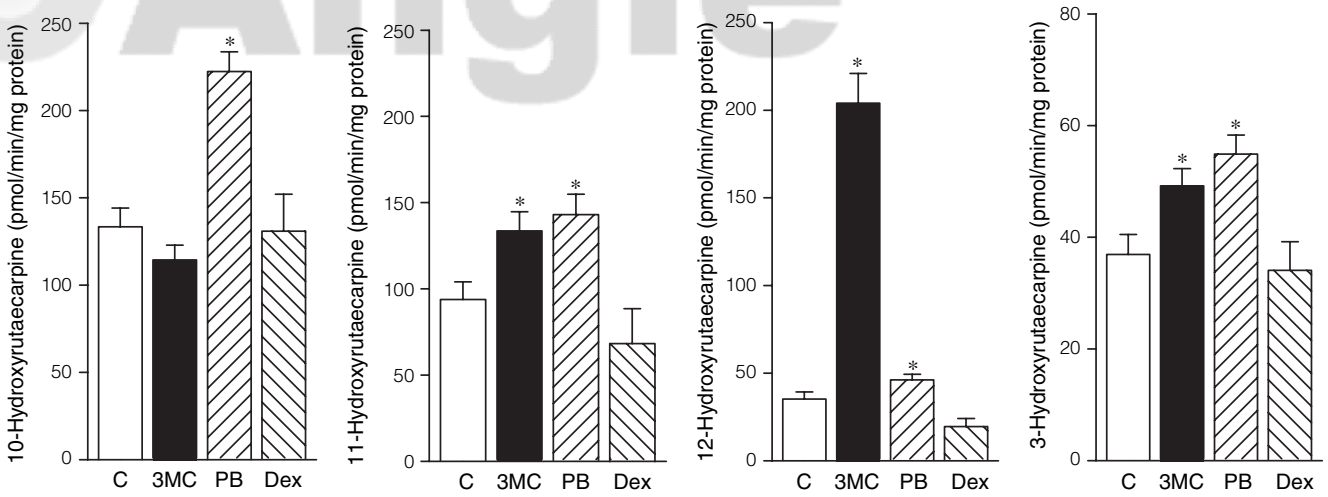

Figure 4. Effects of P450 inducers on mouse liver microsomal rutaecarpine hydroxylation activities. Liver microsomes of control (C) (□), 3-methylcholanthrene (3MC)- (■), Phenobarbital (PB)- (▨), and dexamethasone (Dex)- (▧) treated mice were prepared and rutaecarpine hydroxylation activities were determined. Results represent the mean ± SEM of four mice. *Asterisks represent values significantly different from the control value, $p < 0.05$.

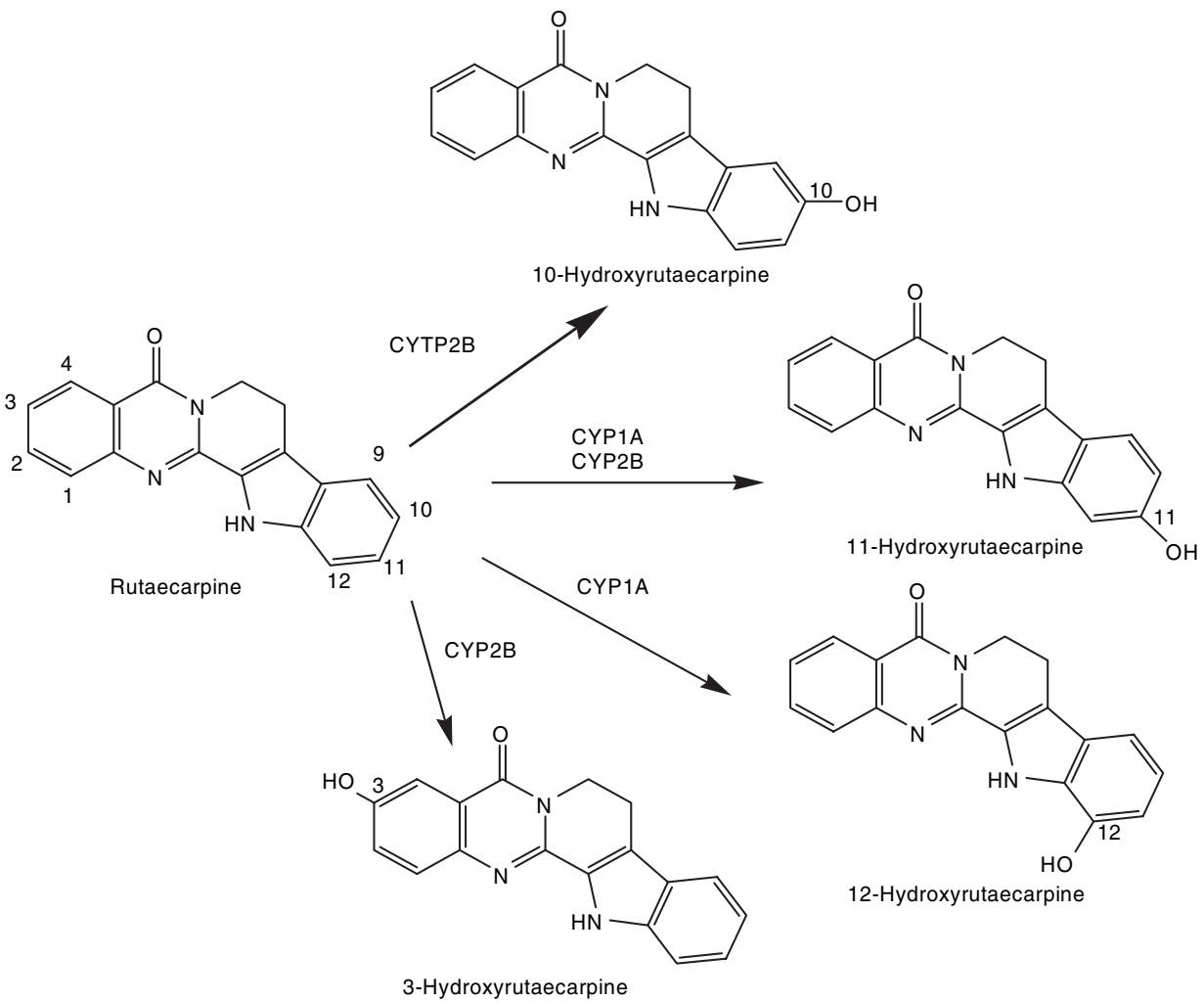

Figure 5. Rutaecarpine hydroxylation by mouse P450 forms.

Kinetic analysis showed that V_{max} values for mouse rutaecarpine hydroxylation ranged from 62 to 197pmol/min/mg protein (Table 1 and Figure 3); K_m values for rutaecarpine hydroxylation ranged from 11.6 to 16.7 μM in untreated mouse liver microsomes; V_{max} value for 10-hydroxylation was slightly elevated over 11-hydroxylation value; and K_m values for 10- and 11-hydroxylation were similar. A Lineweaver-Burk plot revealed a linear pattern without the presence of a two-phase pattern of high and low affinity enzymes (Figure 3B). In rats, CYP1A and CYP2B play major roles in catalyzing rutaecarpine hydroxylation[9]. Similar to hydroxylations in rats, our induction and inhibition results also demonstrated that CYP1A and CYP2B were the main P450 forms involved in mouse rutaecarpine hydroxylations. We have also identified the P450 forms that participated in each hydroxylation. 3-MC-inducible 11-, 12-, and 3-hydroxylations were highly sensitive to the α-NF inhibition (Table 2 and Figure 4); phenobarbital-inducible 10-, 11-, 12-, and 3-hydroxylations were inhibited by orphenadrine (Table 2 and Figure 4); and phenobarbital-treatment increased both CYP2B and CYP3A activities[20]. Dexamethasone and ketoconazole were found to have no effects on rutaecarpine hydroxylation activity (Table 2 and Figure 4). These results indicate a crucial role for both CYP1A and CYP2B in rutaecarpine 11-, 12-, and 3-hydroxylation (Figure 5) and a crucial role for CYP2B in rutaecarpine 10-hydroxylation. In untreated mouse liver microsomes, CYP1A2 was the only CYP1A member detectable by the immunoblot analysis[7]. Our previous report showed an IC_{50} value for rutaecarpine in human CYP1A2 much lower than that in human CYP1A1[5]. Among CYP1A members, CYP1A2 may play a primary role in mouse hepatic rutaecarpine hydroxylation. On the contrary, 10-hydroxylation was inhibited by α-NF but not induced by 3-MC. In addition to CYP1A, α-NF was found also to inhibit other P450 forms such as CYP2C[21]. However, rutaecarpine hydroxylation activities were not affected by sulfaphenazole, a CYP2C inhibitor, at 10 μM (Table 2). Increasing the concentration of sulfaphenazole to 100 μM, we obsereved rutaecarpine 10-, 11-, 12-, and 3- hydroxylation activities were at 88%, 104%, 113%, and 84%, respectively, of control values, indicating that sulfaphenazole at 100 μM did not significantly inhibit rutaecarpine hydroxylation activities either. The reasons for inhibition inconsistencies with induction data are not clear. Additional studies, such as immunoinhibition, may provide further evidence for the involvement of P450 forms.

In summary, our results show that 10- and 11-hydroxyrutaecarpine are the major microsomal oxidation metabolites of rutaecarpine in mice (Table 1 and Figure 1). The results of our induction and inhibition studies demonstrated that mouse rutaecarpine hydroxylations were mainly catalyzed by CYP1A and CYP2B (Figure 5). To obtain a better application of *E. rutaecarpa*, the pharmacological effects of hydroxyrutaecarpines must be studied further to assess the possible influences on these effects of P450 modulators (e.g., flavonoids, barbiturates, and cigarette smoking).

ACKNOWLEDGEMENTS

This work was supported by NSC 91-2320-B077-010 and the National Research Institute of Chinese Medicine.

REFERENCES

1. Liao, J. F., Chen, C. F. and Chow, S. Y. 1981. Pharmacological studies of Chinese herbs. 9. Pharmacological effects of *Evodiae fructus*. J. Formosa Med. Assoc. 79: 30-38.
2. Tang, W. and Eisenbrand, G. 1992. *Evodia rutaecarpa* (Juss) Benth. In "Chinese Drugs of Plant Origin". pp. 509-514. Tang, W. and Eisenbrand, G. eds. Springer-Verlag, Berlin.
3. Sheu, J. R. 1999. Pharmacological effects of rutaecarpine, an alkaloid isolated from *Evodia rutaecarpa*. Cardiovas. Drug Rev. 17: 237-245.
4. Hasler, J. A., Estabrook, R., Murray, M., Pikuleva, I., Watreman, M., Capdevila, J., Holla, V., Helvig, C., Falck, J. R., Farrell, G., Kaminsky, L. S., Spivack, S. D., Boitier, E. and Beaune, P. 1999. Human cytochrome P450. Mol. Aspec. Med. 20: 1-137.
5. Ueng, Y. F., Jan, W. C., Lin, L. C., Chen, T. L., Guengerich, F. P. and Chen, C. F. 2002. The alkaloid rutaecarpine is a selective inhibitor of cytochrome P450 1A in mouse and human liver microsomes. Drug Metab. Dispos. 30: 349-353.
6. Iwata, H., Tezuka, Y., Kadota, S., Hiratsuka, A. and Watabe, T. 2005. Mechanism-based inactivation of human liver microsomal CYP3A4 by rutaecarpine and limonin from Evodia fruit extract. Drug Metab. Pharmacokinet. 20: 34-45.
7. Ueng, Y. F., Wang, J. J., Lin, L. C., Park, S. S. and Chen, C. F. 2001. Induction of cytochrome P450-dependent monooxygenase in mouse liver and kidney by rutaecarpine, an alkaloid of the herbal drug *Evodia rutaecarpa*. Life Sci. 70: 207-217.
8. Ueng, Y. F., Yu, H. J., Lee, C. H., Peng, C., Jan, W. C., Ho, L. K., Chen, C. F. and Don, M. J. 2005. Identification of microsomal oxidation metabolites of rutaecarpine, a main active alkaloid of the medicinal herb *Evodia rutaecarpa*. J. Chromatogr. A 1076: 103-109.
9. Lee, S. K., Kim, N. H., Lee, J., Kim, D. H., Lee, E. S., Choi, H. G., Chang, H. W., Jahng, Y. and Jeong, T. C. 2004. Induction of cytochrome P450s by rutaecarpine and metabolism of rutaecarpine by cytochrome P450s. Planta. Med. 70: 753-757.
10. Waxman, D. J. 1999. P450 gene induction by structurally diverse xenochemicals: Central role of nuclear

receptor CAR, PXR, and PPAR. Arch. Biochem. Biophys. 369: 11-23.
11. Fontaine, S. M., Hoyer, P. B. and Sipes, I. G. 2001. Evaluation of hepatic cytochrome P4502E1 in the species-dependent bioactivation of 4-vinylcyclohexene. Life Sci. 69: 923-934.
12. Waxman, D. J. and Azaroff, L. 1992. Phenobarbital induction of cytochrome P-450 gene expression. Biochem. J. 281: 577-592.
13. Balawin, S. J., Bloomer, J. C., Smith, G. J., Ayrton, A. D., Clarke, S. E. and Chenery, R. J. 1995. Ketoconazole and sulphaphenazole as the respective selective inhibitors of P450 3A and 2C9. Xenobiotica 25: 261-270.
14. Bourrie, M., Meunier, V., Berger, Y. and Fabre, G. 1996. Cytochrome P450 isoform inhibitors as a tool for the investigation of metabolic reactions catalyzed by human liver microsomes. J. Pharmacol. Exp. Ther. 277: 321-332.
15. Bergman, J. and Bergman, S. 1985. Studies of rutaecarpine and related quinazolinocarboline alkaloids. J. Org. Chem. 50: 1246-1255.
16. Alvares, A. P. and Mannering, G. J. 1970. Two substrate kinetics of drug-metabolizing enzyme systems of hepatic microsomes. Mol. Pharmacol. 6: 206-212.
17. Lowry, O. H., Roseborough, N. J., Farr, A. L. and Randall, R. L. 1951. Protein measurement with the Folin phenol reagent. J. Biol. Chem. 193: 265-275.
18. Omura, T. and Sato, R. 1964. The carbon monoxide-binding pigment of liver microsomes. 1. Evidence for its hemeprotein nature. J. Biol. Chem. 239: 2370-2379.
19. Guengerich, F. P. 1997. Comparisons of catalytic selectivity of cytochrome P450 subfamily enzymes from different species. Chem. Biol. Interact. 106: 161-182.
20. Mäkinen, J., Frank, C., Jyrkkärinne, J., Gynther, J., Carlberg, C. and Honkakoski, P. 2002. Modulation of mouse and human phenobarbital-responsive enhancer module by nuclear receptors. Mol. Pharmacol. 62: 366-378.
21. Chang, T. K. H., Gonzalez, F. J. and Waxman, D. J. 1994. Evaluation of triacetyloleandomycin, α-naphthoflavone and diethyldithiocarbamate as selective chemical probes for inhibition of human cytochromes P450. Arch. Biochem. Biophys. 311: 437-442.